

Plasma-assisted atomic layer deposition of Al_2O_3 and parylene C bi-layer encapsulation for chronic implantable electronics

Xianzong Xie,¹ Loren Rieth,¹ Srinivas Merugu,¹ Prashant Tathireddy,¹
and Florian Solzbacher^{1,2}

¹Department of Electrical and Computer Engineering, University of Utah, Salt Lake City, Utah 84112, USA

²Department of Bioengineering, University of Utah, Salt Lake City, Utah 84112, USA

(Received 11 July 2012; accepted 14 August 2012; published online 27 August 2012)

Encapsulation of biomedical implants with complex three dimensional geometries is one of the greatest challenges achieving long-term functionality and stability. This report presents an encapsulation scheme that combines Al_2O_3 by atomic layer deposition with parylene C for implantable electronic systems. The Al_2O_3 -parylene C bi-layer was used to encapsulate interdigitated electrodes, which were tested *in vitro* by soak testing in phosphate buffered saline solution at body temperature (37 °C) and elevated temperatures (57 °C and 67 °C) for accelerated lifetime testing up to 5 months. Leakage current and electrochemical impedance spectroscopy were measured for evaluating the integrity and insulation performance of the coating. Leakage current was stably about 15 pA at 5 V dc, and impedance was constantly about 3.5 M Ω at 1 kHz by using electrochemical impedance spectroscopy for samples under 67 °C about 5 months (approximately equivalent to 40 months at 37 °C). Alumina and parylene coating lasted at least 3 times longer than parylene coated samples tested at 80 °C. The excellent insulation performance of the encapsulation shows its potential usefulness for chronic implants. © 2012 American Institute of Physics. [<http://dx.doi.org/10.1063/1.4748322>]

There continues to be a strong interest in developing biomedical implantable devices, such as cochlear implants,¹ diaphragm pacing systems,² and deep brain stimulators for treating diseases such as hearing loss, respiratory failure, and Parkinson's.³ Neuroprosthetics systems require chronic implantation of neural interfaces able to perform for years or decades to reduce surgical risks from follow-up surgeries and generate levels of efficacy that justifies the risks associated with the implants. The device has to be protected from the harsh body environment, which allows device to perform its intended use. Therefore, encapsulation of implantable device is critical to its functionality, stability, and longevity. Wireless systems have been widely developed because they typically have less foreign body response than tethered (wired) devices.⁴ Soft encapsulation has been preferred for implantable devices over hermetic encapsulation based on metal canisters due to limited space and interference with telemetry communication, especially for wireless systems. The encapsulation has to be biocompatible, conformal, and highly resistive and have a low dielectric constant.⁵ Parylene C (Refs. 6–8) has been widely used as encapsulation material for different kinds of implantable devices, based on its low water absorption rate of 0.1% for 24 h,⁹ low dielectric constant of 3.15 at 60 Hz,⁹ USP Class VI biocompatibility, and chemical inertness. Parylene C is also an excellent ion barrier,¹⁰ which makes it very attractive for implantable devices. Failure of parylene C encapsulation has been reported¹¹ due to moisture diffusion and interface contamination. Reactive parylene has been developed by adding functional group to improve the adhesion and short-term insulation performance⁸; however, this does not keep water moisture from penetration. In order to prevent this from happening, moisture has to be isolated from the interface with the coated devices.

Otherwise, moisture will condense around hygroscopic interface contaminants, causing devices failure.

Atomic layer deposited (ALD) Al_2O_3 has been demonstrated as an excellent moisture barrier^{12,13} with water vapor transmission rate (WVTR) of 10^{-6} g/m²·day, for preventing degradation of extremely moisture-sensitive organic light emitting diodes (OLEDs). ALD Al_2O_3 is superior compared with films generated by other deposition techniques such as sputtered Al_2O_3 as a moisture barrier^{12,14} because it is highly conformal and pin-hole free. Liquid water is known to corrode Al_2O_3 (Ref. 15); therefore, Al_2O_3 film alone is not suitable for encapsulation of biomedical implants exposed directly to the body environment. The idea of combining Al_2O_3 and parylene is based on the concept that Al_2O_3 works as an inner moisture barrier and parylene as external barrier to ions and prevents contact of Al_2O_3 with liquid water, and to inhibit the transport of reactants/products involved with corrosion of the Al_2O_3 layer.

In this letter, we are reporting the *in vitro* performance of the bi-layer encapsulation scheme based on interdigitated electrodes (IDEs) described below. IDEs coated with 52-nm of plasma-assisted (PA) ALD Al_2O_3 and 6 μm of parylene C had leakage currents of 15 pA and impedance of 3.5 M Ω at 1 kHz after being soaked in $1\times$ phosphate buffered saline (PBS) at 37 °C for approximate 5 months without any obvious change. Accelerated soaking tests were also performed at elevated temperature (57 °C, 67 °C, and 80 °C). 80 °C is considered a high temperature for soak testing of polymer materials and might activate new failure modes, compromising the predictive power of those measurements. The measurements are quite useful as a worst-case scenario, since activation of additional failure modes would likely only decrease the device lifetime. Electrochemical impedance

spectroscopy (EIS) and chronoamperometry were performed by Gamry potentiostat (Gamry instruments) to monitor the performance of the encapsulation. IDE test structures were fabricated using standard lift-off lithographic techniques on 500- μm thick fused silica substrate. Electrodes were 130 μm wide with the same spacing in between. The electrodes were composed of Ti(100 nm)/Pt(150 nm)/Au(150 nm) sequentially to match the metallization used for wireless version of Utah Electrode Arrays (UEAs),¹⁶ which are comprised of 10 by 10 silicon-based electrodes with Ti/Pt/Au backside metal for flip-chip bonding. The IDEs were then annealed at 375 °C in forming gas (98% of Ar and 2% of H₂) for 45 min. Two lead wires were soldered to two bond pads on IDEs for electrical contact (Fig. 1). Thin Al₂O₃ films were deposited using plasma assisted atomic layer deposition (PAALD) by sequentially exposing IDEs to trimethylaluminum (TMA) vapor and oxygen plasma for 500 cycles at 120 °C using Fiji F200 (Cambridge NanoTech Inc.). The PAALD cycle consisted of 0.06 s TMA pulse, 10 s argon purge (200 SCCM), 20 s O₂ plasma (20 SCCM), and 5 s argon purge (200 SCCM) at 0.3 mTorr. PAALD process was preferred for its lower deposition temperature and shorter purge time comparing with a thermal ALD process. Also, PAALD reduces hydrogen incorporation in Al₂O₃ films compared to thermal ALD,^{17,18} thus improving the film quality.^{18,19} The deposition rate was about 1.04 Å/cycle on silicon substrate, measured by using VASE ellipsometer (J.A. Woollam Co., Inc), which is similar to Langeris *et al.* reported.¹³ Following the PAALD layer, 6 μm of parylene C were deposited using the standard Gorham process in LabTop 3000 parylene coater (Para Tech Coating).⁹ Silane A-174 (Momentive Performance Materials) was employed as adhesion promoter for the interface between Al₂O₃ and parylene C. IDEs were soaked in 6-ml vials (Fig. 1) with 1× PBS

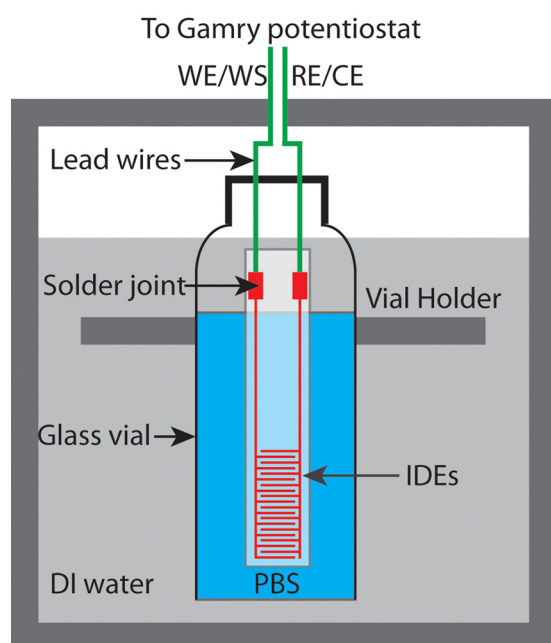


FIG. 1. Schematic of soak testing setup. Two lead wires were soldered to two microfabricated big bond pads on the IDEs for electrical connection, and they came out of the vial through a pre-drilled small hole on the cap. The impedance and leakage current measurements were conducted using a two-electrode configuration by connecting the working sensing to working and counter to reference electrodes, respectively.

in a customized soaking chamber. The PTFE insulation at the end of lead wires was removed for the purpose of electrical connection to the Gamry potentiostat. PBS was changed every other week to minimize the ion concentration change due to water evaporation. All the leakage current and impedance measurements were done in 1× PBS solution under pre-set constant temperature.

AFM micrographs show that the Al₂O₃ film (RMS surface roughness of 0.17 nm for the fused silica substrate) has RMS surface roughness of 0.48 nm, as shown in Figure 2, indicating highly conformal and uniform film. X-ray photoelectron spectroscopy (XPS) was used to measure the composition of Al₂O₃ films for as deposited and depth profiled samples. The measurements were collected using a Kratos AxisUltraDLD instrument with monochromatic Al-K α radiation, and Ar-ion sputtering for depth profiling using 4 kV ions. The measured compositions are presented in Table I, and show an O/Al ratio of as-deposited Al₂O₃ films was 1.41, compared to a stoichiometric value of 1.5. Previous reports in the literature have measured an O/Al ratio of >2.^{12,20} No Ar gas was measured by XPS in the film.

Impedance of the encapsulation and its changes with time are very important because it is inversely related to crosstalk and signal loss via shunting with biological fluids, especially for implants with active electronics. EIS is widely utilized to evaluate the longevity and degradation kinetics of coatings.^{21,22} Wide spectrum (1 Hz–1 MHz) impedance was measured to provide more information regarding the overall performance of the encapsulation. Impedance was first measured in air before soaking (Figure 3). The measurement results were fitted into a simple constant phase element (CPE) equivalent circuit model based on the relative constant phase. Capacitance of the dry IDEs was about 45 pF. The phase was almost constant at 90° for the whole frequency range, indicating the expected purely capacitive behavior. Then samples were soaked in 1× PBS at 37 °C. Impedance dropped about one order of magnitude immediately after the sample was immersed in PBS, and the phase stayed almost constant (90°) at high frequency (>100 Hz) and increased about 5° at low frequency (1–100 Hz). Thereafter, the impedance and phase remained nearly unchanged during the 140-

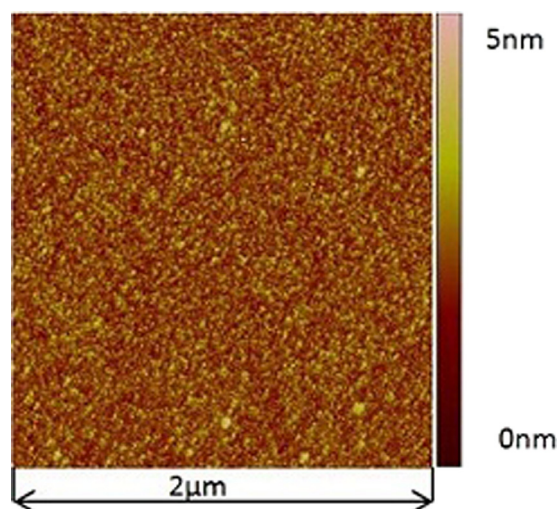


FIG. 2. AFM micrograph of as-deposited 52 nm of Al₂O₃ on quartz substrate.

TABLE I. XPS analysis of an Al_2O_3 layer deposited using PAALD process-500 cycles of TMA + O_2 gas on fused silica.

Etch time(s)	O 1s	C 1s	Al_2p	Si_2p
0	51.5	14.5	34	0
300	57.3	0.5	42.2	0
600	58.5	0	41.5	0
900	57.8	0	41.9	0.3
1200	13.2	1.4	7.8	77.6
1500	0.9	0	0	99.1

day soak testing. The consistency of the impedance indicated that the encapsulation was intact. The capacitance based on the CPE model was about 66 pF, which was about a 50% increase compared to measurements in air. This is most likely due change of ambient media from air to PBS. Water has relative permittivity of 80,²³ which is much higher than of parylene C ($\epsilon_r = 3.15$) and air. This would increase the “equivalent” relative permittivity of the coating, and thus the capacitance of the test structures.

Accelerated lifetime test was performed in order to expedite the validation process of this encapsulation scheme as the films need to encapsulate the devices for years at 37 °C.⁷ Body temperature (37 °C) has been chosen as a baseline, and accelerated aging factors (F) are listed in Table II based on a doubling of the reaction rate for each 10 °C increase.^{24,25} Impedance and phase of IDEs soaked at different temperatures were almost identical (Figure 4). During the 140-day period of soaking test, samples at higher temperature were expected to fail faster based on Arrhenius equation. No significant changes in the EIS data from degradation in the encapsulation have been observed as expected in most cases since the encapsulation is still almost intact and it is far from failure. Because of this, the accelerated lifetime testing is not able to resolve the characteristics of the encapsulation degradation at this time and determine if they have an Arrhenius character.

The impedance of the encapsulation at 1 kHz is important for a lot of applications, e.g., neural recording and stimulation,

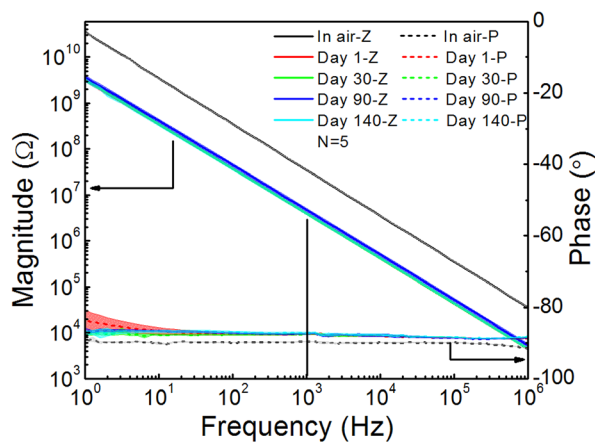


FIG. 3. Bode plots of impedance spectroscopy of 140-day soaking test in 37 °C PBS for alumina and parylene C coated samples. The magnitude was denoted by Z and the phase was denoted by P in the legend. Data was acquired from 5 (N refers to number of samples) samples and shaded areas represent the standard error. There was an initial drop for the impedance from air to PBS; then the impedance and phase remained nearly constant.

TABLE II. Accelerated aging factors and equivalent soaking time for different elevated temperatures relative to 37 °C.

Temperature (°C)	Aging factor (F)	Real soaking time (day)	Equivalent soaking time at 37 °C (day)
37	1	140	140
57	4	140	560
67	8	140	1120
80	20	57	1140

because the frequency of action potentials is about 1 kHz. Figure 5 shows the impedance of IDEs soaked at different temperatures at 1 kHz. The impedance was initially about 36 MΩ for all samples in air; it dropped to 3.5 MΩ immediately after immersion in PBS and remained at the same level for the rest of the testing period. This impedance is very high, which is a very good insulation for implantable electronics. This is about one order of magnitude higher than Hsu *et al.*⁷ (IDEs with same dimensions used) and Seymour *et al.*⁸ reported by using parylene C as encapsulation and also Hsu *et al.*⁷ reported using a-SiC_x:H encapsulation.²⁶ The factor that could possibly contribute the high impedance is that fused silica has higher resistivity than silicon substrate.²⁷

Leakage current is another important metric for the performance of encapsulation and was measured by continuously applying 5 V dc bias. The temperature-voltage bias should have significant effect on accelerated failures.²⁸ Figure 6 shows the leakage current of IDEs soaked at different temperatures. The leakage current was about 1 pA for all the samples in air before soaking; it increased dramatically to about 15 pA (approximately equivalent to $3.3 \times 10^{11} \Omega$ dc resistance) immediately after being soaked and then remained almost unchanged for the rest of the soaking period for alumina and parylene coated samples. For parylene coating, the leakage current increased dramatically up to nA range after 130 days of soaking at 57 °C, indicating failure of the coating. The parallel dc resistance from CPE modeling ranged from 10^{11} to $5 \times 10^{11} \Omega$, which was consistent with the leakage current measured. The initial current increase is mainly because of the dc resistance drop. When IDEs are in air, the effective

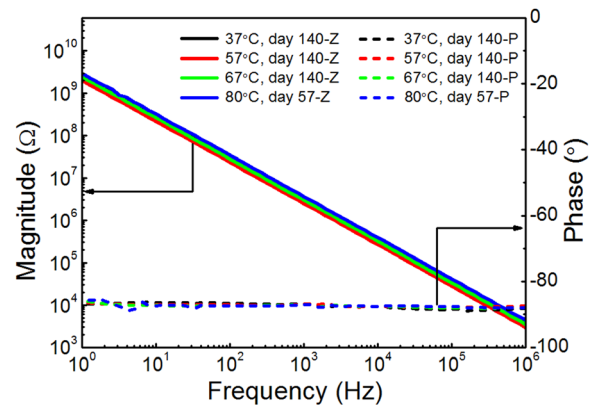


FIG. 4. Impedance spectroscopy plots of IDEs at 37 °C and elevated temperature for accelerated testing in PBS. The magnitude was denoted by Z and the phase was denoted by P in the legend. The time in the plot is the actual soaking time at that specific temperature. No obvious temperature effect has been observed yet. Soak testing of the presented samples continued after the publication of this report.

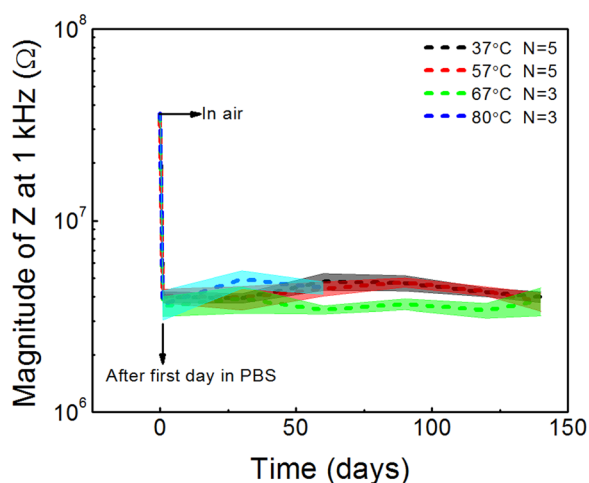


FIG. 5. Magnitude of impedance at 1 kHz for IDEs soaked at different temperatures in PBS. N refers to number of samples. "Day 0" means samples were in air before soak testing.

distance for dc resistance was $130\ \mu\text{m}$ (distance between two electrodes); after being soaked in PBS, it became about $12\ \mu\text{m}$ (2 $6\text{-}\mu\text{m}$ thick parylene layer and conductive PBS). The effective distance for dc resistance decreased about 10 times, which leads to the dramatic increase in leakage current. The consistency of leakage current suggests that no obvious corrosion was occurring to the Al_2O_3 film. The extremely low leakage current ($\leq 20\text{ pA}$) was excellent for IDEs after roughly three years of equivalent soaking time at 37°C . We have to keep in mind that planar test structures tend to have longer lifetime compared with integrated devices for a couple of reasons: (1) complex topography, (2) force from micromotion of the device after being implanted, (3) tethering force from wires of the device, (4) damage due to handling/implantation during surgery. Those factors are not fully presented or activated with IDE test structures. Testing of fully integrated devices with alumina and parylene coating is under way.

In conclusion, we have demonstrated that combination of PAALD Al_2O_3 and parylene C has excellent insulation performance for test structures and is a promising near-hermetic encapsulation for implantable microsystems and electronics. IDEs coated with Al_2O_3 and parylene C were

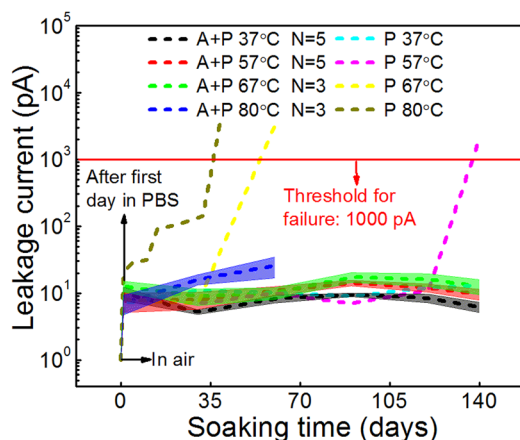


FIG. 6. Leakage current test plots of 140-day test period for parylene (P) coating and alumina and parylene (A+P) coating under 5 V dc bias. N refers to number of samples. "Day 0" means samples were in air before soaking test.

tested at 37°C and elevated (57 to 80°C) temperatures (about three years of equivalent soaking time at 37°C) in PBS and the impedance kept at $3.5\ \text{M}\Omega$ and leakage current was at around 15 pA . The initial impedance drop and leakage current increase were analyzed. Temperature effect on the lifetime of the IDEs was studied, and equivalent lifetime was roughly estimated. Alumina and parylene coating lasted at least 3 times longer than parylene coated samples at 80°C , showing its robustness and superiority. Those results demonstrated the quite excellent potential suitability of combining with Al_2O_3 and parylene C as encapsulation for chronic biomedical implants. Long-term *in vivo* test of the encapsulation needs to be performed to further justify this encapsulation scheme.

This work was supported in part by DARPA (Contract No. N66001-06-C-4056) and NIH (Contract No. 1R01NS064318-01A1). The authors gratefully acknowledge Charles Fisher at the Nanofab of the University of Utah for his help of Al_2O_3 deposition. Florian Solzbacher has commercial interest in Blackrock microsystems, which manufactures and sells neural interfaces. The views expressed are those of the authors and do not reflect the official policy or position of the Department of Defense or the U.S. Government. Approved for Public Release, Distribution Unlimited.

- ¹N. R. Peterson, D. B. Pisoni, and R. T. Miyamoto, *Restor. Neurol. Neurosci.* **28**(2), 237 (2010).
- ²D. E. Weese-Mayer, A. S. Morrow, R. T. Brouillette, M. N. Ilbawi, and C. E. Hunt, *Am. J. Respiratory Critical Care Med.* **139**(4), 974 (1989).
- ³G. Deuschl, C. Schade-Brittinger, P. Krack, J. Volkmann, H. Schäfer, K. Bötzel, C. Daniels, A. Deutschländer, U. Dillmann, and W. Eisner, *New England J. Med.* **355**(9), 896 (2006).
- ⁴R. Biran, D. C. Martin, and P. A. Tresco, *J. Biomed. Mater. Res. Part A* **82**(1), 169 (2007).
- ⁵P. de Vos, M. Bucko, P. Gemeiner, M. Navrátil, J. Svitel, M. Faas, B. L. Strand, and G. Skjak-Braek, *Biomaterials* **30**(13), 2559 (2009).
- ⁶C. Hassler, R. P. von Metzen, P. Ruther, and T. Stieglitz, *J. Biomed. Mater. Res. Part B: Appl. Biomater.* **93**(1), 266 (2010).
- ⁷J. M. Hsu, L. Rieth, R. A. Normann, P. Tathireddy, and F. Solzbacher, *IEEE Trans. Biomed. Eng.* **56**(1), 23 (2009).
- ⁸J. P. Seymour, Y. M. Elkasabi, H. Y. Chen, J. Lahann, and D. R. Kipke, *Biomaterials* **30**(31), 6158 (2009).
- ⁹J. B. Fortin and T. M. Lu, *Chemical Vapor Deposition Polymerization: The Growth and Properties of Parylene Thin Films* (Springer, 2004).
- ¹⁰M. Szwarc, *Polym. Eng. Sci.* **16**(7), 473 (1976).
- ¹¹W. Li, D. C. Rodger, P. R. Menon, and Y. C. Tai, *ECS Trans.* **11**(18), 1 (2008).
- ¹²A. P. Ghosh, L. J. Gerenser, C. M. Jarman, and J. E. Fornalik, *Appl. Phys. Lett.* **86**, 223503 (2005).
- ¹³E. Langereis, M. Creatore, S. B. S. Heil, M. C. M. Van de Sanden, and W. M. M. Kessels, *Appl. Phys. Lett.* **89**(8), 081915 (2006).
- ¹⁴T. T. A. Li and A. Cuevas, *Prog. Photovoltaics: Res. Appl.* **19**(3), 320 (2011).
- ¹⁵A. Abdulagatov, Y. Yan, J. Cooper, Y. Zhang, Z. Gibbs, A. S. Cavanagh, R. Yang, Y. Lee, and S. M. George, *ACS Appl. Mater. Interfaces* **3**(12), 4593 (2011).
- ¹⁶S. Kim, R. Bhandari, M. Klein, S. Negi, L. Rieth, P. Tathireddy, M. Toepfer, H. Oppermann, and F. Solzbacher, *Biomed. Microdevices* **11**(2), 453 (2009).
- ¹⁷M. D. Groner, F. H. Fabreguette, J. W. Elam, and S. M. George, *Chem. Mater.* **16**(4), 639 (2004).
- ¹⁸G. Dingemans, R. Seguin, P. Engelhart, M. C. M. van de Sanden, and W. M. M. Kessels, *Phys. Status Solidi (RRL)—Rapid Res. Lett.* **4**(1–2), 10 (2010).
- ¹⁹K. H. Hwang, in ALD Conference, Monterey, CA, 14 May 2001.
- ²⁰S. K. Kim, S. W. Lee, C. S. Hwang, Y. S. Min, J. Y. Won, and J. Jeong, *J. Electrochem. Soc.* **153**, F69 (2006).
- ²¹E. P. M. Van Westing, G. M. Ferrari, and J. H. W. De Wit, *Electrochim. Acta* **39**(7), 899 (1994).
- ²²E. Akbarinezhad and H. R. Faridi, *Surface Eng.* **24**(4), 280 (2008).

- ²³M. Uematsu and E. U. Franck, *Static Dielectric Constant of Water and Steam* (American Chemical Society and the American Institute of Physics for the National Bureau of Standards, 1981).
- ²⁴K. J. Hemmerich, *Med. Plastic Biomater.* **5**, 16 (1998).
- ²⁵D. W. L. Hukins, A. Mahomed, and S. N. Kukureka, *Med. Eng. Phys.* **30**(10), 1270 (2008).
- ²⁶J. M. Hsu, P. Tathireddy, L. Rieth, A. R. Normann, and F. Solzbacher, *Thin Solid Films* **516**(1), 34 (2007).
- ²⁷X. Z. Xie, L. Rieth, P. Tathireddy, and F. Solzbacher, *Procedia Eng.* **25**, 483 (2011).
- ²⁸J. J. Filliben, *Engineering Statistics Handbook* (National Institute of Standards and Technology, 2007), Chap. 8.